REPORT DOCUMENTATION PAGE

Form Approved
OMB No. 0704-0188

1. AGENCY USE ONLY (Leave blank)	2. REPORT DATE	3. REPORT TYPE AND DATES COVERED
	September 1, 1996	Final, 01/01/92 - 05/31/94

4. TITLE AND SUBTITLE
Spectroscopic Investigations of Nonambient Systems with Millimeter and Submillimeter Probes

5. FUNDING NUMBERS
DAAL03-92-G-0007

6. AUTHOR(S)
Frank C. De Lucia, Department of Physics

7. PERFORMING ORGANIZATION NAME(S) AND ADDRESS(ES)
The Ohio State University Research Foundation
1960 Kenny Road
Columbus, Ohio 43210-1063

8. PERFORMING ORGANIZATION REPORT NUMBER
RF MPN: 769611
PN: 725668

9. SPONSORING MONITORING AGENCY NAME(S) AND ADDRESS(ES)
Department of the Army
U.S. Army Laboratory Command
Army Research Office
P.O. Box 12211
Research Triangle Pk., NC 27709

10. SPONSORING / MONITORING AGENCY REPORT NUMBER
ARO 29324.1-PH

11. SUPPLEMENTARY NOTES

12a. DISTRIBUTION AVAILABILITY STATEMENT

12b. DISTRIBUTION CODE

13. ABSTRACT (Maximum 200 words)

The project, "Spectroscopic Investigations of Nonambient Systems with Millimeter and Submillimeter Probes," addressed a broad range of scientific topics and technological developments important to this spectral region. For the purposes of this discussion, we have divided the report on research results into three parts: (1) Molecular collisional processes from 1 K to 1000 K; (2) Energy transfer in polyatomic molecules; and (3) Development and uses of millimeter and submillimeter technology. Also included is a lists of personnel who worked on these projects and publications.

14. SUBJECT TERMS	15. NUMBER OF PAGES 34
	16. PRICE CODE

17. SECURITY CLASSIFICATION OF REPORT	18. SECURITY CLASSIFICATION OF THIS PAGE	19. SECURITY CLASSIFICATION OF ABSTRACT	20. LIMITATION OF ABSTRACT
UNCLASSIFIED	UNCLASSIFIED	UNCLASSIFIED	

TABLE OF CONTENTS

Abstract	3
I. INTRODUCTION AND BACKGROUND	3
A. The mm/submm Spectral Region	3
B. Applications	4
II. EXPERIMENTAL AND THEORETICAL CONSIDERATIONS	6
A. Gas Phase Molecular Interactions as a Function of Temperature	6
B. System Sensitivity as a Function of Temperature	8
III. RESULTS	9
A. Collisional Processes between 1 K and 1000 K	9
B. Energy Transfer in Polyatomic Molecules	20
C. Millimeter and Submillimeter Technology	29
IV. PARTICIPATING SCIENTIFIC PERSONNEL	30
V. LIST OF PUBLICATIONS	31
V. BIBLIOGRAPHY	33

ABSTRACT OF WORK UNDER ARO CONTRACT DAAL03-92-G-0007

The project, "Spectroscopic Investigations of Nonambient Systems with Millimeter and Submillimeter Probes," addressed a broad range of scientific topics and technological developments important to this spectral region. For the purposes of this discussion, we have divided the report on research results into three parts: (1) Molecular collisional processes from 1 K to 1000 K; (2) Energy transfer in polyatomic molecules; and (3) Development and uses of millimeter and submillimeter technology. Also included is a lists of personnel who worked on these projects and publications.

I. INTRODUCTION AND BACKGROUND

The project addressed the development and use of spectroscopic techniques for the study of molecular systems under nonambient conditions. Emphasis was placed on the use of millimeter and submillimeter spectroscopic methods as diagnostic probes of these environments although many of these techniques are also applicable in other spectral regions. In some cases, the mm/submm spectral region was especially advantageous for the work while in others it was merely convenient because of our experience and equipment base in this part of the spectrum. Much of what is discussed is based upon previous developments in our laboratory. In this Introduction, we will briefly discuss some of the basis for this work; in later sections more of the details and references are provided.

A. The mm/submm Spectral Region

1. The spectroscopic technique: The mm/submm spectroscopic technique which was used in many of these experiments has been developed over a period of years.[1-3] Briefly, nonlinear harmonic generators which produce the mm/submm radiation are driven by klystrons or traveling wave tube amplifiers[4] in the region around 50 GHz. These microwave sources are in turn referenced to or driven by sources which are controlled by frequency synthesizers, effectively giving a synthesized source which is conveniently and continuously tunable throughout the region between ~ 100 - 1000 GHz. This mm/submm energy is radiated quasi-optically through the atomic and molecular system being studied and detected by an InSb detector operating at 1.5 K or a 0.3 K germanium bolometer. Associated electronics are used for frequency measurement and signal recovery. Systems of this type have proven to be reliable, easy to operate, and reasonably inexpensive. Because of these attributes, a number of similar systems have now been built at laboratories around the world and have become the standard for a wide range of molecular

studies in this spectral region.

2. Characteristics of mm/submm spectroscopy: Much of the work discussed in this report depended upon several important attributes of our technique for spectroscopic studies in the mm/submm spectral region. Among these are:

a) It is a very sensitive technique. Under equilibrium conditions, rotational absorption coefficients increase as $\nu^2 \rightarrow \nu^3$ and peak typically in the vicinity of 1000 GHz. Under optimum non-equilibrium conditions, achievable in our pumped experiments, concentrations as small as 100 cm^{-3} (~10^{-14} Torr partial pressure) can be studied with modest signal averaging. Calculations based on a more aggressive set of assumptions yield concentrations as small as 1 cm^{-3}.

b) Because of the broad tunable coverage in the frequency regime that corresponds to many of the rotational transitions of the small, fundamental species that we wish to study, transitions can be chosen on the basis of their diagnostic value rather than to satisfy coincidence criteria. Furthermore, because of the high resolution, spectral overlap is very rare.

c) It is an absorption technique. Because the transitions that are observed are rotational transitions with accurately known transition moments, the absolute absorption data can be accurately converted into molecular information.

d) Because we directly observe rotational transitions, the method is especially sensitive to rotational nonequilibria. For example, at 300 K and 300 GHz a 5 % change in the population of one of the states involved in a transition produces a 100 % change in the observed line strength.

e) Because this is the frequency regime in which a very large number of optically pumped lasers have been discovered, we can take advantage of the hundreds of man years that have been spent searching for CO_2 laser pump coincidences.

B. Applications

Over a number of years we have used these mm/submm techniques for a wide variety of spectroscopic investigations and technical developments. In the sections below some of those that are related to the proposed work are briefly discussed.

1. Spectroscopy of small, fundamental molecular species: The principal initial application of this spectroscopic technique was its use to develop a basic spectroscopic understanding of the rotational spectra of small, fundamental molecules. Particular emphasis was placed on species of atmospheric, astronomical, chemical, and spectroscopic interest. This work has included studies of light asymmetric rotors such as H_2O and H_2S, prototype internal rotors such as HOOH and CH_3OH, light asymmetric rotors with electronic angular momenta such as NO_2, HO_2, and HCO, and a number of unstable species and ions such as CCH, NO^+, and LiH. In addition to the exper-

imental aspects of this work, we have also developed theoretical and computational methods for characterizing to microwave accuracy these spectra over wide spectral ranges. Many (if not most) of these studies were the first to provide characterization of these species to microwave accuracy over large portions of their rotational spectra in the mm/submm. This work is of importance to the reported work because the basic spectroscopic properties (energy levels, transition frequencies, transition moments, etc.) of the molecular species which we studied first had to be well understood.

2. Collisionally cooled spectroscopy at very low temperatures: As is discussed in more detail in Section III, we have devoted a significant portion of our effort toward the development and exploitation of a collisional cooling technique which provides a simple method for the study of gas phase processes at temperatures down to about 1 K.[5-8] The scientific motivation for this work has been the desire to study molecular interactions in the regime where $kT \leq h\nu_r$. In this regime the rotational energy levels play a much more intimate role in the collisional process. This technique has now allowed us to study pressure broadening continuously over the 1 - 1000 K regime as well as vibrational and rotational relaxation. We have found that the mechanisms responsible for broadening and relaxation make a transition from being dominated at high temperature by semi-classical inelastic collisions to domination in the lower energy regime by resonances associated with quasibound states. The variety and richness of the results that we have obtained have been beyond our expectations.

3. Ion spectroscopy: Several years ago we reported a new technique for the study of molecular ions which used an axial magnetic field to extend the negative glow region of an abnormal glow discharge to produce increases of ion density of one to two orders of magnitude with corresponding increases in observed signal strength.[9] We have also used this method for a number of mm/submm studies and it has been widely adopted by the spectroscopic community, with similar systems having been built at a number of locations including Berkeley, Wisconsin, Harvard, Lille, and Giessen.[10-14] In a new system we have combined this technique with collisional cooling for the study of molecular ions at very low temperatures. This new system provides a significant new nonambient environment for our studies, but at least as importantly provides a path to experiments with more independent control of the environmental parameters such as partial pressures of constituents, electron flux, ion concentration, and temperature. Some results from this system are shown in Section III.

4. Collisional Energy Transfer: For a number of years we have also had an interest in the internal mechanisms of molecular lasers and the collisional energy transfer processes that are the basis of them.[15-20] Our emphasis has been on rotational processes both because this degree of freedom corresponds most closely with mm/submm devices and because a number of interesting basic problems exist in rotational energy transfer.

II. EXPERIMENTAL AND THEORETICAL CONSIDERATIONS IN NONAMBIENT ENVIRONMENTS

Because the thrust of this report is the study of molecular systems under nonambient conditions, it is useful to briefly consider the spectroscopic consequences of significant changes in temperature both on spectroscopic parameters and the physics of the systems being studied.

A. Gas Phase Molecular Interactions as a Function of Temperature

First consider the temperature scaling laws for the interaction of gas phase molecular systems and mm/submm radiation. For the purposes of numerical comparison, we will assume that a system originally at 300 K is cooled to 4 K and that it may be diluted in a collisional cooling gas.

1. Linewidth: In the mm/submm spectral region experiments are typically run at or near Doppler broadened limits. Since Doppler broadening is proportional to $T^{1/2}$, linewidths at 4 K are typically an order of magnitude narrower and correspondingly greater resolution and measurement accuracy are possible. In addition, since sensitivity is ordinarily determined by peak, not integrated intensity, this factor under many circumstances also adds an order of magnitude to system sensitivity. We have confirmed this expectation in a number of studies.[5,6,7,8,21-24]

2. Sensitivity: Several temperature dependent factors affect molecular absorption coefficients. The rotational absorption coefficient is given by

$$\alpha = [8\pi^2\nu/3ch] \cdot |\langle m|\mu|n\rangle|^2 \cdot [N/\Delta\nu] \cdot [1-e^{-h\nu/kT}] \cdot [1/Q_r]$$

where it has been factored to separate the individual temperature dependent terms. The behavior of $N/\Delta\nu$ depends upon the details of the pressure broadening, but simple theory gives

$$N/\Delta\nu \propto T^{-1/2}$$

Q_r is the rotational partition function which approaches 1 in the low temperature limit. If we consider molecules whose $J = 0 - 1$ transitions fall at ~ 100 GHz, Q_r at 300 K is ~ 100 - 1000. The term $[1-e^{-h\nu/kT}]$, which represents the difference between induced absorption and emission varies between unity in the limit $h\nu >> kT$ and ~1/100 for transitions of ν ~ 100 GHz at 300 K. Together these factors represent a four or five order of magnitude gain in absorption coefficient for systems at very low temperature.

Other factors are more dependent on the details of the system. The dilution ratio of the

spectroscopic gas in the cooling gas will reduce this gain for stable species, but the reduced pressure broadening parameters associated with zero dipole moment collision partners and the gains in detector sensitivity for low background environments will add to the overall system gains. The latter factor will be especially significant when detector noise is the limiting factor in the system. To give two typical examples, the absorption coefficients of gas phase CO and HCN at 4 K are 25 cm^{-1} and 10000 cm^{-1} respectively. Thus, we conclude that even at very large dilutions of the spectroscopic species in the collisional cooling gas, absorption coefficients will be very large. Again, this expectation has been confirmed in our recent work and molecules with small dilution ratios (~ 10^{-4} - 10^{-6}) are easily observable on an oscilloscope screen in real time.

3. Physics: The spectral complexity of many systems is considerably reduced at low temperature. For example, it has been elegantly demonstrated by many workers using free jet expansions that the complexity of rotational structure in room temperature spectra can be dramatically simplified.[25,26] Collisional cooling has the additional attributes of macroscopic path lengths and independently measurable, adjustable temperature.

In addition, rotational collisional processes are of both fundamental and practical importance and many articles and reviews on the subject have been written. In a review article, Brunner and Pritchard[27] compare and contrast 'photon' spectroscopy and 'collisional' spectroscopy. They point out that both spectroscopies are characterized (in principle) by massive amounts of data (mostly redundant) that should be calculable from a relatively small number of 'spectroscopic' constants. However, the nature of 'collisional' spectroscopy is such that it is much more difficult to invert the problem so that fundamental parameters may be recovered from the experimental results. Even if these parameters are given, it is usually a formidable computational task to calculate the effects of these collisions either for the comparison of experiment and theory or for use in other problems. This is because of the participation of the very large number of thermally accessible rotational states in each collision process and because of the increased complexity of molecule-molecule/atom interactions in comparison with molecule-field interactions. The dynamics of the interplay between theory and experiment are further hindered by the nature of the available experimental data. Fundamental parameters are recoverable from most experimental data only via complex (and usually unrealizable) deconvolutions. The origin of this difficulty is very similar to the cause of the theoretical complexity, the large number of thermally populated states and the nature of the molecular interaction. Thus, it is expected that the very large reduction in the number of thermally populated states at low temperature will make the relation between observables and the fundamental interactions substantially more direct. Results which support this expectation are reported in Section III. This is one of the principal motivations for our work. Finally, these very low temperatures significantly enhance the production and lifetime of weakly bound complexes such as van der Waals molecules and also

provide additional opportunities for the study of ions and other transient species.

B. System Sensitivity as a Function of Temperature

Over much of the mm/submm spectral region, the sensitivity of our experimental technique is directly proportional to the sensitivity of the detector employed. The cooled detectors used in our work approach being ideal detectors in that their NEP's approach being limited by the fluctuations in the blackbody radiation that is incident on them along with the spectrometer signal. In fact, if one of these detectors is completely broadband and can view the entire 300 K blackbody spectrum, its NEP is limited to about 5×10^{-11} W/Hz$^{1/2}$. In the mm/submm the use of cooled filters that only pass the long wavelength portion of the 300 K blackbody along with the spectrometer signal can significantly improve this. For a cutoff frequency of ν_m the NEP for an ideal broadband detector is given in the long wavelength limit by NEP ~ $kT\nu_m^{1/2}$.[28] For a ν_m = 1000 GHz, this corresponds to ~ 10^{-15} W. The 1.5 K InSb detectors that we have used in these systems for many years[29] have NEP's in the range of 10^{-12} - 10^{-13} W/Hz$^{1/2}$ and the 0.3 K ^{3}He detector mentioned above has a NEP of the order 2×10^{-15} W/Hz$^{1/2}$, about 50 times better. It is our experience that this has added a similar amount to our system performance. However, the equation above shows that the construction of a more sensitive broadband detector for the mm/submm spectral region is not possible if it must view a room temperature experiment.

III. RESULTS

A. Pressure Broadening Spectroscopy from 1 K to 1000 K

As discussed briefly above, it is possible to consider collisional processes as a 'spectroscopy' in which a large number of observables (e. g. the cross sections as a function of temperature) are related to a smaller number of molecular parameters which are ultimately related to the intramolecular potential. However, as is well known, this is not as straightforward as in energy level spectroscopy for a host of reasons. These range from substantially increased theoretical and computational difficulty to real questions about the sensitivity of the observables to the underlying parameters which govern the processes. In this section we show recent experimental and theoretical results which address these issues. *An important theme which emerges is that these questions are most interesting at low temperatures.*

1. Experimental results (neutrals): To date we have investigated the helium and hydrogen pressure broadening characteristics as a function of temperature for a number of species including CO, NO, CH_3F, H_2S, DCl, H_2O, HDO, OCS, SO_2, and CH_2F_2.[5,6,7,8,21,22,23,30-36] Our development of the collisional cooling technique was motivated by both the general ideas discussed above as well as a desire to carry out specific experimental investigations. In general, we wanted to be able to experimentally investigate a regime for which $h\nu_r \geq kT$; thus having molecular systems in analogy to atoms at room temperature, with the energy level spacing large compared to kT. However, only part of the analogy between molecules at very low temperature and atoms under ambient conditions holds because at very low temperatures the collision energies are small or comparable to van der Waals binding energies. Thus, the molecular systems have the additional features of systems that can form quasibound states at very low temperature.[37-39] As a consequence, a rich spectrum of results has been observed that is dependent on the spectroscopic species, its rotational state, and the collision partner.

Before showing experimental results, it is worthwhile discussing some of the qualitative features that should be expected. Although it is always dangerous to ascribe too physical a picture to process that are inherently nonclassical, doing so provides in this case a good mechanism for classifying and understanding the results of our experiments. In the semi-classical picture (valid at higher temperature) of molecular collisions and their contributions to line broadening, the energy defect (which is a measure of the energy that is transferred between internal and external degrees of freedom) and its relation to kT play important roles. Whenever this defect becomes too large, the efficiency of the collisions in producing broadening and/or inelastic collisions is reduced; and, in the limit of zero translational energy, this efficiency also becomes zero. However, an additional effect can become important in very low energy collisions. Because of the existence of shallow (tens of cm^{-1} for collisions with He) attractive wells in the intermolecular

potential, resonances in both the pressure broadening and inelastic cross sections associated with quasibound states can exist. Some of these open channels with significant cross section result from interactions which involve rotational levels which lie at low enough energy to interact with the shallow wells. Others depend solely on the shape of the intermolecular potential between the collision partners. Because these shallow attractive wells extend to large radius, for very low energy collisions very large cross sections can result.

Thus, in the limit of small collision energy there are two countervailing effects; the reduction in cross section due to the growth in the energy defect and the increase in cross section due to the low energy resonances. Because both of these effects are sensitive functions of the intermolecular potential and the energy level structure of the molecule, a wide variety of functional dependencies of cross section on temperature are expected. These qualitative expectations have been borne out by diagnostic calculations of Palma and Green for the CO - He system,[40] by a number of calculations which we have done using the MOLSCAT routines of Green and Hutson, and by the experimental results shown below.

Figures III.A.1 and III.A.2 serve as good illustrations. Both show two important qualitative features: the clear transition between the semiclassical and quantum regimes and the large difference between the cross sections for He and H_2 collisions at low temperature. As expected from semiclassical theory, for collisions with both He and H_2 there are large regimes of constant or nearly constant cross section above 100 - 200 K. However, only for the He - H_2S system is the expected drop in semiclassical cross section at lower temperature observed. We will show below that the physical parameters of the other systems are such that regions of efficient semi-classical and quantum broadening overlap, thereby obscuring the decrease in semi-classical cross section.

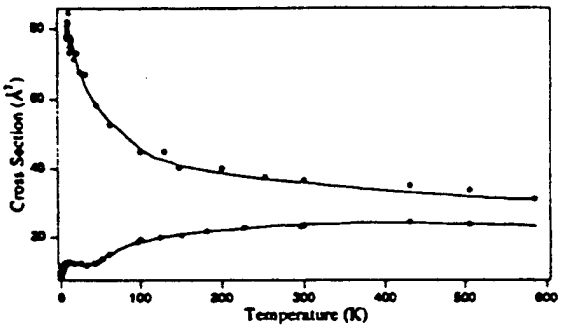

Figure III.A.1. Pressure broadening cross sections for H_2 (upper) and He (lower) collisions with H_2S between 2 and 600 K.

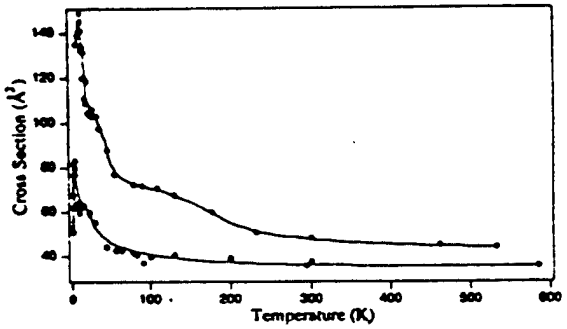

Figure III.A.2. Pressure broadening cross sections for H_2 (upper) and He (lower) collisions with CH_3F between 2 and 600 K.

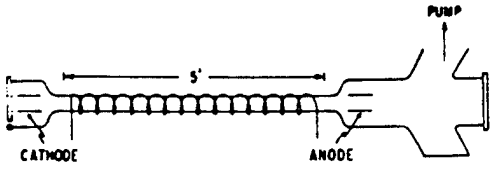

Figure III.A.3. System for the enhanced production of molecular ions via the magnetically lenghtened negative glow region of an abnormal glow discharge.

2. Experimental Results (molecular ions):

One of our goals has been to develop and exploit techniques for the study of collisions with molecular ions over the 1 - 1000 K range, especially at the lower temperatures.

In order to consider the new system we have developed for these studies, it is first useful to review the technique which we developed several years ago for the production and study of molecular ions.[9] This system, shown in Fig. III.A.3, is based on the magnetic confinement and axial extension of the negative glow region of a low pressure discharge. In it the usual glass discharge cell with internal cylindrical electrodes is placed inside a solenoid and cooled to 77 K. Figure III.A.4 shows the dramatic increase in signal strength with increasing magnetic field in this system. This two order of magnitude increase has resulted in it being widely adopted by the spectroscopic community for the study of molecular ions.[10,11,12,13,14] The essence of the

method is that the ion rich negative glow region of an abnormal[41] glow discharge, when operated in an axial magnetic field of a few hundred gauss, lengthens from its usual length of a few millimeters to fill the entire length of the cell. Under these conditions the cathode drop region is in essence a source of ~1 keV electrons which are injected into the electric field free,

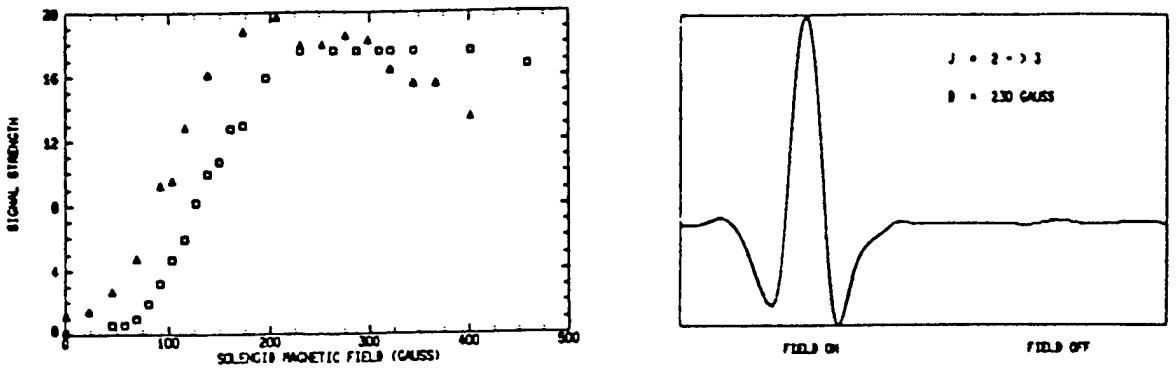

Figure III.A.4. Observed linestrength for the J = 2 - 3 transitions of HN_2^+ and HCO^+ as a function of axial magnetic field(left). Observed HN_2^+ line with and without magnetic field (right).

magnetically confined negative glow. In this region the electrons slowly lose energy by interactions with the background gas, but because of the magnetic field, the electrons are confined to spiral axially rather than scatter to the walls as in an ordinary discharge. Beyond the confining magnetic field the self sustaining positive column begins. Under ordinary circumstances, it is this ion poor positive column which fill most of the length of the discharge cell. According to this picture, it should be possible to sustain this magnetically confined negative glow inside a metallic tube, because, unlike the positive column, it does not require an electric field gradient to sustain itself.

The system shown in Fig. III.A.5 was developed to test this hypothesis and provide a means for the study of collisions of molecular ions and neutral at very low temperatures. In this system the liquid nitrogen cryogenics which cool the solenoid are separated from the cryogenics which maintain the cell temperature. Additionally, the part of the cell that would contain the electric field free negative glow is made of a conductor (both electrical and thermal) in order to make possible a number of the experiments discussed below.

Consider as a specific example, the H_2 - CO - HCO^+ system. At 77 K both of the precursors have significant vapor pressure; thus if the cell and the solenoid are maintained at 77 K, and if the hypothesis presented above is correct, the basic operation of this system should coincide with the operation of the glass system shown in Fig. III.A.3. Our tests of this system have shown the

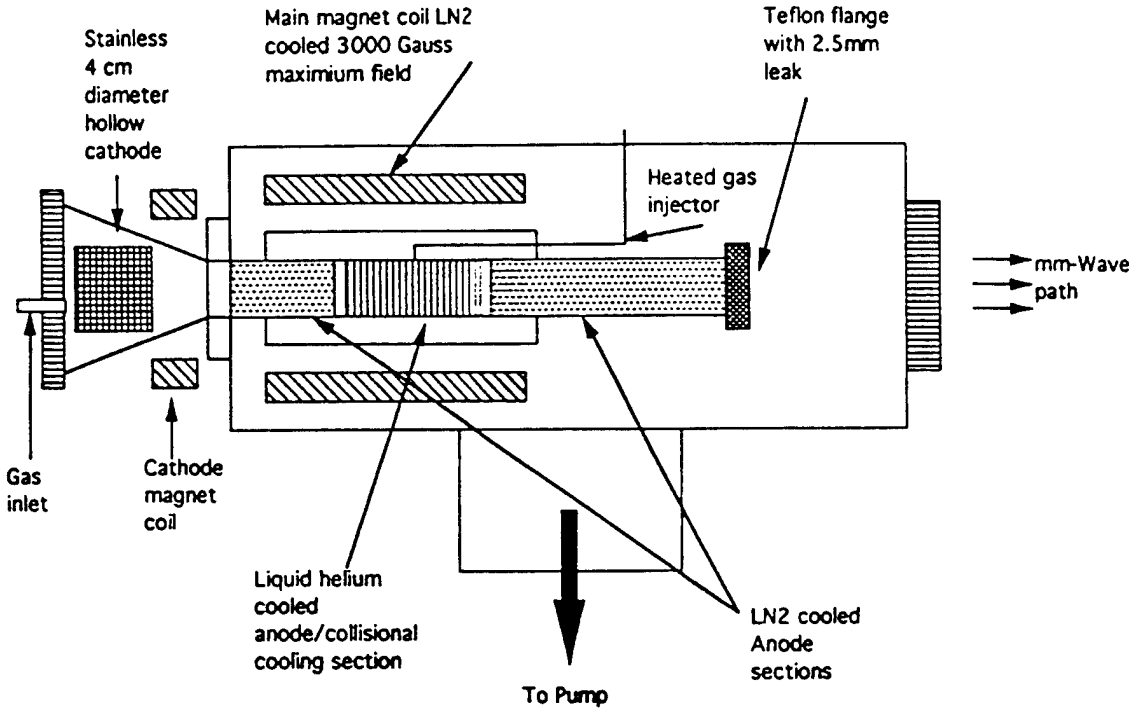

Figure III.A.5 System for the study of molecular ions at very low temperature.

hypothesis to be correct, with a graph of signal strength as a function of magnetic field similar to that shown in Fig. III.A.4. To use this system (or any discharge system) for collisional studies, it is necessary to have an understanding of the temperature distribution and discharge induced chemistry in the discharge. Additionally, in order to work at very low temperatures it is necessary to incorporate into the system an efficient helium collisionally cooled cell. Both of these requirements are greatly aided because the voltage drop across the negative glow region is very small (basic discharge theory yields zero). Thus, the energy deposition here is very low. More specifically, of the ~10 Watts of discharge power (1 keV @ 10 ma), the vast majority is either deposited at the cathode or anode, with a vanishingly small portion being deposited in the helium cooled spectroscopic region. Furthermore, because the spectroscopically active molecules are injected and subsequently trapped in the helium region, essentially all of the probed molecules and molecular ions exist only in this cryogenic region.

Never-the-less it is imperative to independently measure the effects of the discharge on the temperature. One of the reasons for this is that heat capacities decrease dramatically at helium temperatures; thus, small energy inputs can lead to temperature increases. We have adopted two,

complementary methods to address this issue: a calibration based on the measured cross section of collisionally cooled CO (which can be observed in the absence of a discharge in this and other systems), and a zero point extrapolation in current, both for the CO and the HCO^+ itself. Our measurements show that under typical operating conditions (~10 ma discharge current) broad regimes exist in which quantitative collisional studies can be carried out. These have been described in detail in a recent publication.[42]

3. Theory and discussion: As a basis for a consideration of the more complex low temperature regime, let us first consider briefly the higher temperature regime where most previous measurements of the pressure broadening of polyatomic molecules have been done because of vapor pressure considerations. In this semi-classical regime it has been found that the temperature variation of pressure broadening cross sections can ordinarily be characterized by the relation [43]

$$\sigma(T) = \sigma(T_0)\,(T/T_0)^n$$

Thus, even though in principle the cross sections can exhibit complex behavior as the energy defects of the collision channels change in relation to the temperature, they do not in the temperature regimes ordinarily investigated.

Figures III.A.1 and III.A.2 show for collisions with He that above ~100 - 200 K, the cross sections are essentially constant, corresponding to the case n = 0 in the equation above. This is a result which we have also found in studies of a number of other species including H_2O, HDO, and SO_2.[31,32,33,34] It is interesting (but perhaps not too surprising) that the simple physics of these circumstances is well described by the general observation and basic theory of Van Vleck and Weisskopf[44] in which 'hard shell' collisions effect pressure broadening of constant cross section. Additionally, because of the lack of internal degrees of freedom in He, the elegantly simple limit of Anderson Theory [45] presented by Townes and Schawlow[46] gives a more microscopic view, which also provides for a transition from the high temperature to low temperature regime. In this view, the measure of the broadening effectiveness of the Fourier components of the collision is given by a parameter $k = (2\pi b/v)\ \nu_{ab}$ (which in effect compares the molecular transition frequency ν_{ab}, with the fundamental Fourier component of the collision $v/2\pi b$) , where b is the impact parameter, v the molecular velocity and ν_{ab} the rotational transition frequency of the hypothetical two level molecule. For He at 300 K, $2\pi b/v \sim 10^{-12}$, thus providing broadening efficiency for all of the low J levels of the spectroscopically observed species. However, for H_2S at temperatures below ~200 K, the reduced extent of this Fourier spectrum begins to lessen the broadening efficiency of the collisions and the cross section begins to drop. For collisions with CH_3F and CO, this regime of constant cross section extends to

below 50 K as a result of the access of the Fourier components of the collision to the more closely spaced rotational levels of these species. Since for collisions involving He (as well as H_2) well depths are typically tens of wave numbers, pressure broadening cross sections in this higher energy regime are not significantly affected by these wells in the intermolecular potential nor by the phenomena associated with them.

However, for collisions with H_2 below about 150 K, independent of the spectroscopic molecule and transition observed, deviations from the simple power law theory given above have been observed in all species studied.[31,33,34] Again, in the context of semi-classical theory, these deviations are not unexpected, because the rotational energy level spacing in H_2 are comparable to the thermal quanta and the complete semi-classical theories which include the internal degrees of freedom of both collision partners must be used.

At lower temperatures, new phenomena associated with resonances involving quasibound states become important and numerous calculations have shown that cross sections are especially sensitive to the intermolecular potential at low temperatures.[37,38,39,40,47] Figures III.A.1 and III.A.2 show that the cross sections for collisions with both H_2 and He vary rapidly at low temperature. In this regime quantum scattering approaches to pressure broadening become appropriate. In these calculations 'exact' numerical methods which use intermolecular potentials (ordinarily obtained by *ab initio* methods), such as those employed by the MOLSCAT routines of Green and Hutson[48], become appropriate.

At low temperature two parameters have first order impact on the observed cross sections: the depth of the well in the intermolecular potential and the spacing of the rotational energy levels. It is interesting to investigate each of these independently in the context of the CO - He system. Palma and Green[40] have investigated the dependence on well depth. They calculated two additional sets of cross sections in which the depth of the attractive well of the CO - He potential used in the earlier work[49] was first reduced by one half and finally completely eliminated. These are shown in Fig. III.A.6. Figure III.A.7 shows the corresponding family of calculations in which the intermolecular potential is held constant at the *ab initio* value, but in which the energy level spacing is varied. Inspection of these figures show that the results of reducing the well depth or increasing the rotational spacing are similar: a significant reduction in

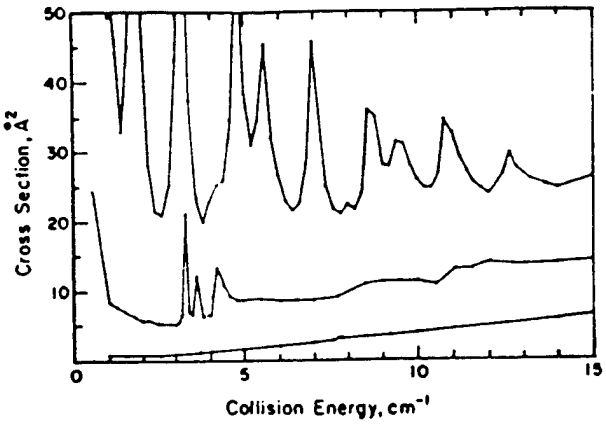

Figure III.A.6. Theoretical pressure broadening cross sections for the J = 0 - 1 line of CO. From top to bottom the curves represent well depths of 1.0, 0.5, and 0.0 times the ab initio value.

the number and strength of the resonances. Many of the resonances in the pressure broadening cross sections shown here can be identified with collision induced rotational state changes. As a consequence, increasing the rotational energy level spacing increases the collisional energy of the resonance; eventually raising the required energy beyond that which the interaction with the shallow well can efficiently supply. Figure III.A.7 also shows for CO - He the resonances in the pressure broadening spectrum are blended

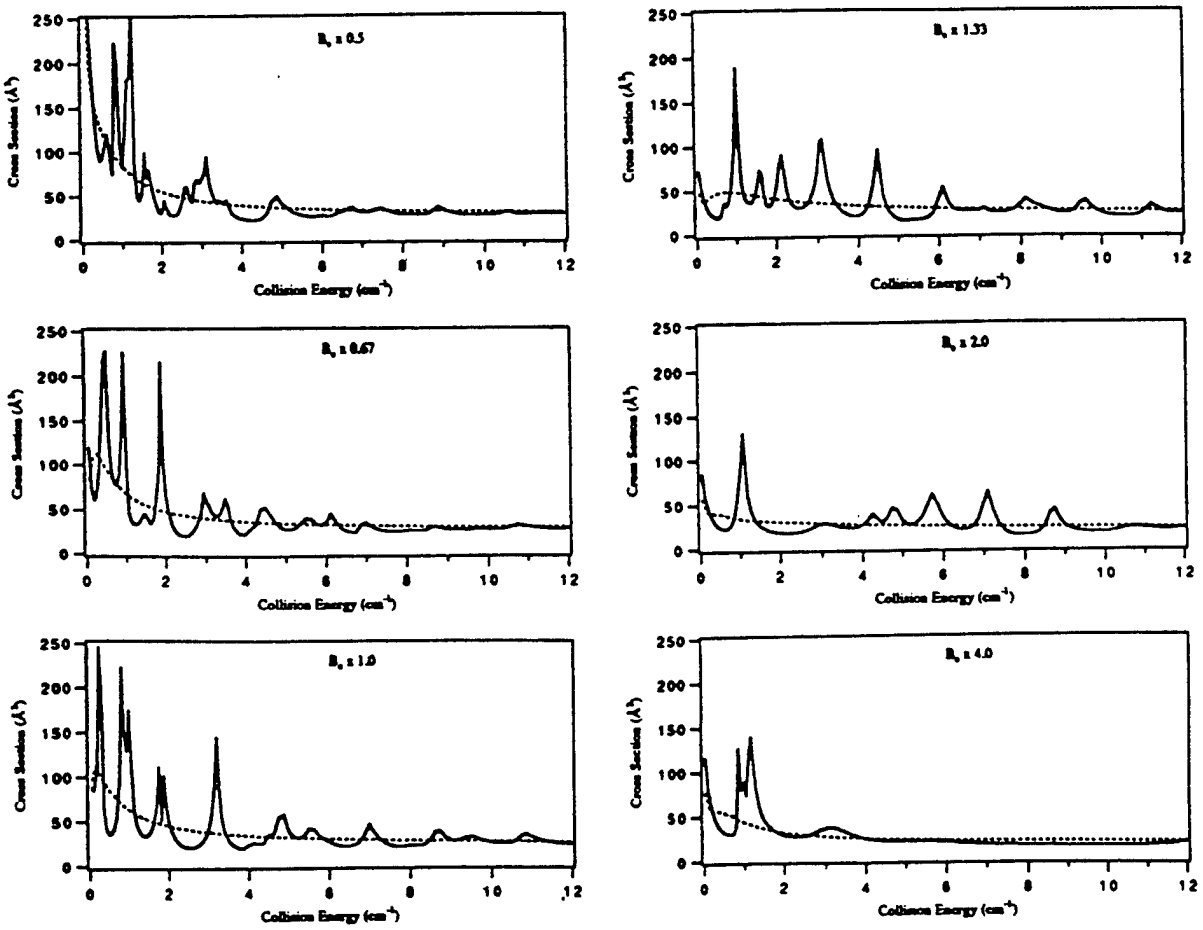

Figure III.A.7. Calculated pressure broadening cross sections for the J = 0 - 1 line of CO. The smooth lines represent the thermal average with T(K) = 1.5 E (cm^{-1}).

together by the thermal average, resulting in a significant reduction in information content. Because these resonances can be associated with *different* state-to-state processes, measurement of these rates can effectively deconvolve them, even in the thermal average. Additionally, closer inspection of Fig. III.A.7, shows that a few of the resonances (e. g. the resonance near 1 cm^{-1}) are largely unaffected by the variation in B. These depend on the shape of the intermolecular potential.

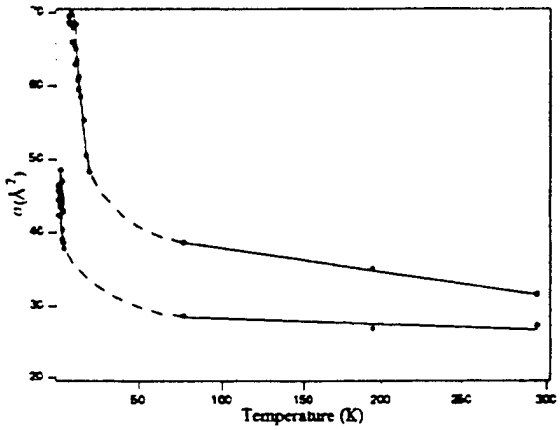

Figure III.A.8. Pressure broadening cross section for the H_2 (upper) and He (lower) collisions with CO. The dashed line is interpolated between the currently available experimental points.

For comparison Fig. III.A.8 shows experimental results for the CO - He as well as CO - H_2 systems. Comparison of these figures shows general agreement between theory and experiment for the J = 0 - 1 transition of the CO - He system. However, the experimental results for the 1 - 2 and 2 - 3 transition lie below the calculated values at low temperature.[5]

Table III.A.1 provides a means for understanding the relationship between the experimental and theoretical results discussed here for the CO - He system and the results shown above for collisions of He and H_2 with CH_3F and H_2S.

Table III.A.1

	Freq (GHz/K)	Well Depth (K)[50]	
		He	H_2
CO (0-1)	115/5.7	19	35
CH_3F (0-1)	51/2.6	62	114
H_2S (1_{10}-1_{01})	168/8.4	58	107

First, because for all species the well depth for collisions with H_2 is about twice as deep as for collisions with He, the interactions which lead to resonances can begin at about twice the

collision energy. Furthermore, because of the relatively closely spaced rotational levels, resonances will exist once they become energetically possible, translating directly the increased well depth into an increase in cross section at about twice the collision energy for collisions with H_2 as for He.

Next, consider the experimental cross sections for collisions between He and H_2S shown in Fig. III.A.1. At about 50 K the decrease in cross section is halted, presumably by the onset of phenomena associated with the attractive well and quasibound states. As for CO - He collisions, this increase in cross section begins around a temperature which corresponds to the well depth, ~60 K.[50] At the lowest temperatures, the cross section begins to drop rapidly once more due to the energetic unavailability of collisional channels involving the relatively widely spaced rotational levels of H_2S. This effect is even larger than implied by Table III.A.1 (which shows only the lowest frequency transition) because the next lowest transition in this light asymmetric rotor is much higher. For collisions between H_2S and H_2, similar considerations lead to quite different results. Because at high temperatures the phenomena associated with the internal degrees of freedom of H_2 which lead to the modest increase in cross section with decreasing temperature are well known, we will not elaborate on them here. However, it is important to note that because of the smaller mass of H_2 the Fourier spectrum of the collision extends to higher energy at a given temperature, and correspondingly, the drop in semi-classical cross section will begin at a lower temperature. More significantly, the attractive well for collisions with H_2 is about twice as deep (~110 K) as for collisions with He. Thus, for collisions with H_2 the temperature regimes for semiclassical and quantum broadening overlap and provide a monotonically increasing cross section. Additionally, the deeper well is more effective in involving the widely spaced rotational levels of H_2S in the creation of pressure broadening resonances at low temperature.

Finally, the most striking qualitative difference between CH_3F and H_2S is the low temperature behavior for collisions with He. None-the-less this difference is readily understood in the context of Table III.A.1 which shows the much larger energy level spacing in H_2S, which closes many of the collision channels at low T. This effect can also be seen in the calculations shown in Fig.III.A.7 where in the energy level spacing is doubled. This effect is much smaller for collisions with H_2 because of its much deeper well.

Because we have a particular interest in HDO, we have also done calculations on this system. Figure III.A.9 shows the calculated pressure broadening cross section below 20 cm^{-1} for two HDO transitions. Because of the widely spaced levels and geometry of this light hydride there are many fewer resonances and significant variation between these transitions, even after a thermal average.

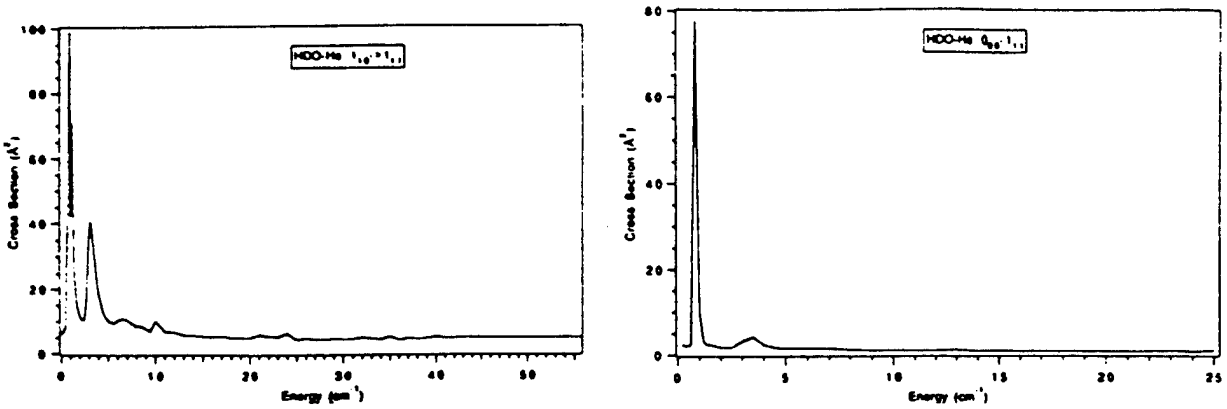

Figure III.A.9. Calculated helium pressure broadening cross sections for (left to right) the $1_{10} - 1_{11}$, and $1_{11} - 0_{00}$ transitions of HDO.

4. Summary: We have shown by a combination of experimental data and theoretical calculations that at low temperature there are two first order effects which determine the qualitative nature of the pressure broadening cross sections: The depth of the attractive well in the intermolecular potential and the rotational energy level spacing. Additionally, we have argued that there is significant information content in the overall functional dependence of this cross section over the general 1 - 1000 K region and that it is reasonable to consider a collisional 'spectroscopy.' At higher temperature, the collision energy in a rather simple picture provides Fourier components which probe the collisional system. At lower temperatures the collisional process cannot be separated into a probe and a system, but rather must be considered quantum mechanically as a whole. None-the-less, the spectroscopy here is more interesting (but also less intuitive) because of the resonances associated with the quasi-bound states.

It remains to be shown: (1)How much information is available from the measurement of the temperature dependence of the pressure broadening cross section for several *different* rotational transitions and how much of it is independent; (2) How (1) is effected by the rotational energy level spacing and well depth; and (3) If a 'spectroscopy' can be established which ties the observable 'spectra' to a smaller set of spectroscopic constants.

B. Energy Transfer in Polyatomic Molecules

Our work on rotational and fast vibrational energy transfer grew out of an initial interest in constructing models of the internal dynamics of FIR molecular lasers which would include modern ideas of molecular collision dynamics. Although the number of degrees of freedom in these molecular systems might at first glance seem discouraging, we used mm/submm spectroscopic diagnostic techniques to establish *experimentally* the existence of pools of levels which are in equilibrium with each other, thereby substantially simplifying the resulting models. Because of the very high sensitivity of mm/submm spectroscopy to nonthermal rotational populations, this could be done with considerable certainty. Examples of such thermal pools include the equilibria of the vibrational bending modes with the R/T temperature in the HCN discharge FIR laser; all of the J rotational levels within the unpumped K = 1 state of the $^{12}CH_3F$ OPFIR laser; and all of the rotational levels within the unpumped symmetry species of $^{35}CH_3Cl$.[15,16,17,18,19,20] This work has provided a quantitative model of the complex HCN discharge laser system as well as significant advances in our understanding of OPFIR lasers. Perhaps the most interesting practical result of this latter work was the demonstration and theoretical explanation of the operation of an OPFIR laser in a high pressure, small cavity regime that was previously though to be forbidden on rather fundamental grounds.[51]

More recently, one of our goals has been to describe the seemingly complex and diverse state-to-state energy transfer data in the context of physically well founded models with small numbers of parameters, parameters which ideally can be related to or calculated from known molecular properties. To this end we have focus on the symmetric tops CH_3F and CH_3Cl. As we will show below, we have been successful in this endeavor, to include being able to relate parameters not only between isotopes, but also between species. For example, for CH_3Cl we are able to account for 358 distinct (44 different probe transitions, two different pump transitions, and multiple appropriate pressures between 1 mTorr and 1 Torr) measured time responses by use of only six adjustable rotational parameters plus two vibrational parameters to account for vibrational processes which are of the same time scale. We will show below that few, if any, of these six rotational parameters are truly adjustable; being calculable either from fundamental parameters or from our earlier work on CH_3F.

This work is related to other efforts in collisional energy transfer. A number of years ago Oka reviewed collision induced rotational relaxation[52] and reported on his pioneering work as well as on the results of others.[53-56] That work laid out basic 'selection' and 'propensity' rules for rotational collisional energy transfer and presented experimental verification for some of these, especially for those based on spin statistics. Since then, other workers have reported observations of infrared-microwave (ir-mw) double resonance effects.[57-59] Recently, a number of double resonance techniques have been used for quantitative studies of rotational relaxation in

polyatomic molecules.[60-67]

From all of this, it has become clear that vibrational energy transfer and rotational energy transfer are not separate and factorable subjects. This is especially true either when systems have very fast vibrational processes which are therefore convolved with rotational processes or when Coriolis or other mixings give rotation like character to 'vibrational' transitions. A nice example of the latter is the work on isotopes of formaldehyde by Haub and Orr.[63] In another example, we have shown in a quantitative modeling of the HCN FIR discharge laser that a similar Coriolis interaction is the principal dissipative agent for the vibrational state containing the upper laser level.[15]

In the work described below time resolved mm/submm-ir double resonance methods were used to obtain the experimental data which formed the basis for the development of numerical models which characterize the molecular energy transfer. The experimental details as well as the results of these investigations have been published in a number of papers.[16,17,18,19,20,68]

1. Modeling: As a first goal in our modeling of rotational and vibrational energy transfer, we have sought to build the kinds of energy transfer models discussed above that describe the systems in terms of a finite number of individual energy levels and thermal pools along with the energy transfer rates that connect them together. Although the resulting models are too complex for analytical solution, we have found that they may be implemented numerically using relatively simple techniques. In this form nonlinear least squares techniques are used to adjust the rates of the model to match the time resolved data obtained from our experiments. Additionally, we have sought to parametrize the model in terms of rates which can be related to fundamental physical processes. Although this fitting of large amounts of time resolved data directly to physical parameters results in large least squares procedures, the advantages of eliminating intermediate fitting parameters significantly outweigh the computational load.

As an example, Fig III.B.1 illustrates the relevant energy levels and pumps for CH_3Cl. It is important to note that the two different CO_2 laser lines pump significantly different J and K energy levels, with substantially different rotational energies. One measure of the significance of these differences is the rather different appearances of the time response data, even for states in thermal pools. Figure III.B.2 shows some of these data. This result is markedly different from that obtained for CH_3F in which the observed time responses for 'pool' transitions were virtually identical, independent of both pump and isotope. As a result the dynamical data obtained from the time resolved mm/submm-ir double resonance experiments for the two pumps are not strongly correlated and, in fact, have rather different qualitative appearance. However, we will show below that all are part of a single pool and that the apparently more complex behavior can be accounted for in the context of a simple extension of the CH_3F model.

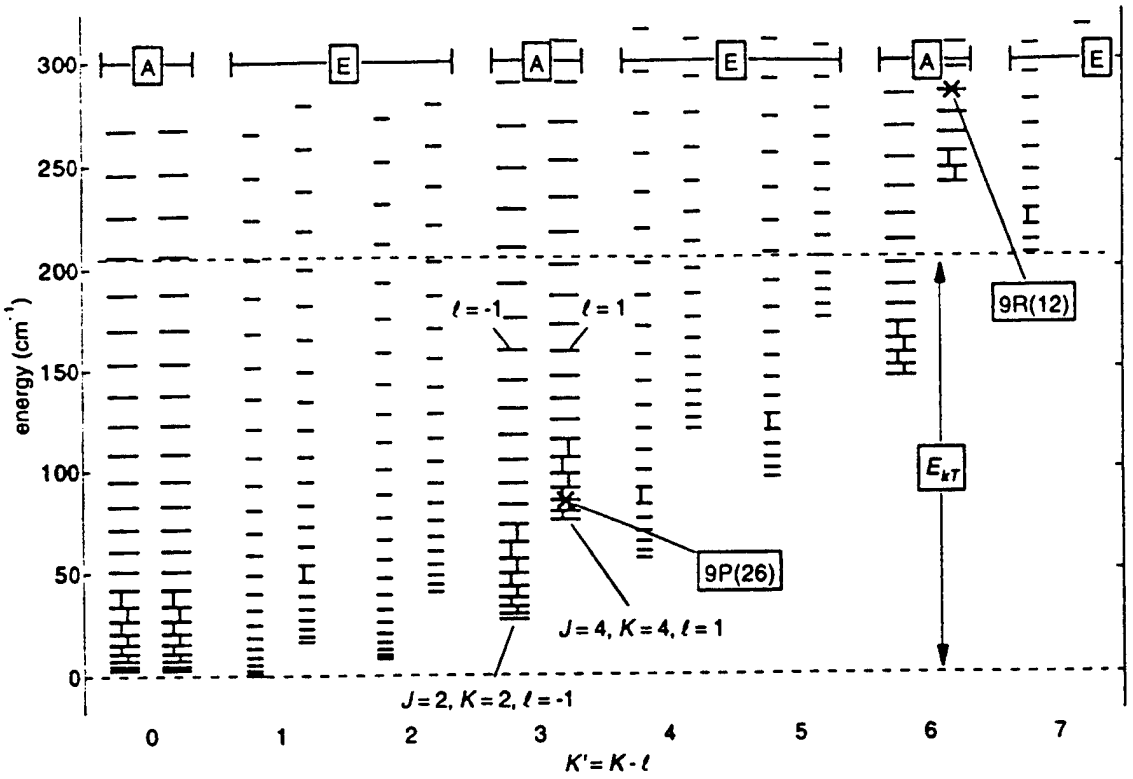

Figure III.B.1. Energy levels and symmetry species of ν_6 vibrational state of CH_3Cl. The states pumped by the CO_2 laser are indicated in the figure.

Briefly, we have found it possible to account for a large and diversified body of experimental data by:

(a) Collecting all of the rotational states of the symmetry species which does not contain the pumped transition into a single thermal pool, with the relative population of the levels within the pool determined by the Boltzmann factor and with the total population and the temperature which describes it free to vary in the model.

(b) Collecting all of the rotational states of the symmetry species which does contain the pumped transition into a similar pool, with the exception of the J states in the pumped K manifold which can have an excess 'nonthermal' population.

(c) Within the pumped K manifold, the nonthermal populations of all J are treated as independent variables. Alternatively, we have found that these populations are described by the Statistical Power Gap (SPG) or Infinite Order Sudden (IOS) theory, with two independent variables describing the state-to-state rates for many levels.

(d) Additional pools for population transfer to vibrational states are included as required by the magnitude of the vibrational excitation. For example in CH_3F for the time resolved mm/submm-ir measurements of energy transfer rates, only the ν_6 is required in addition to the ground vibrational state and the directly pumped ν_3. However, for strongly pumped cw laser systems we have found that population transfer to many additional states profoundly affects the laser operation.[51]

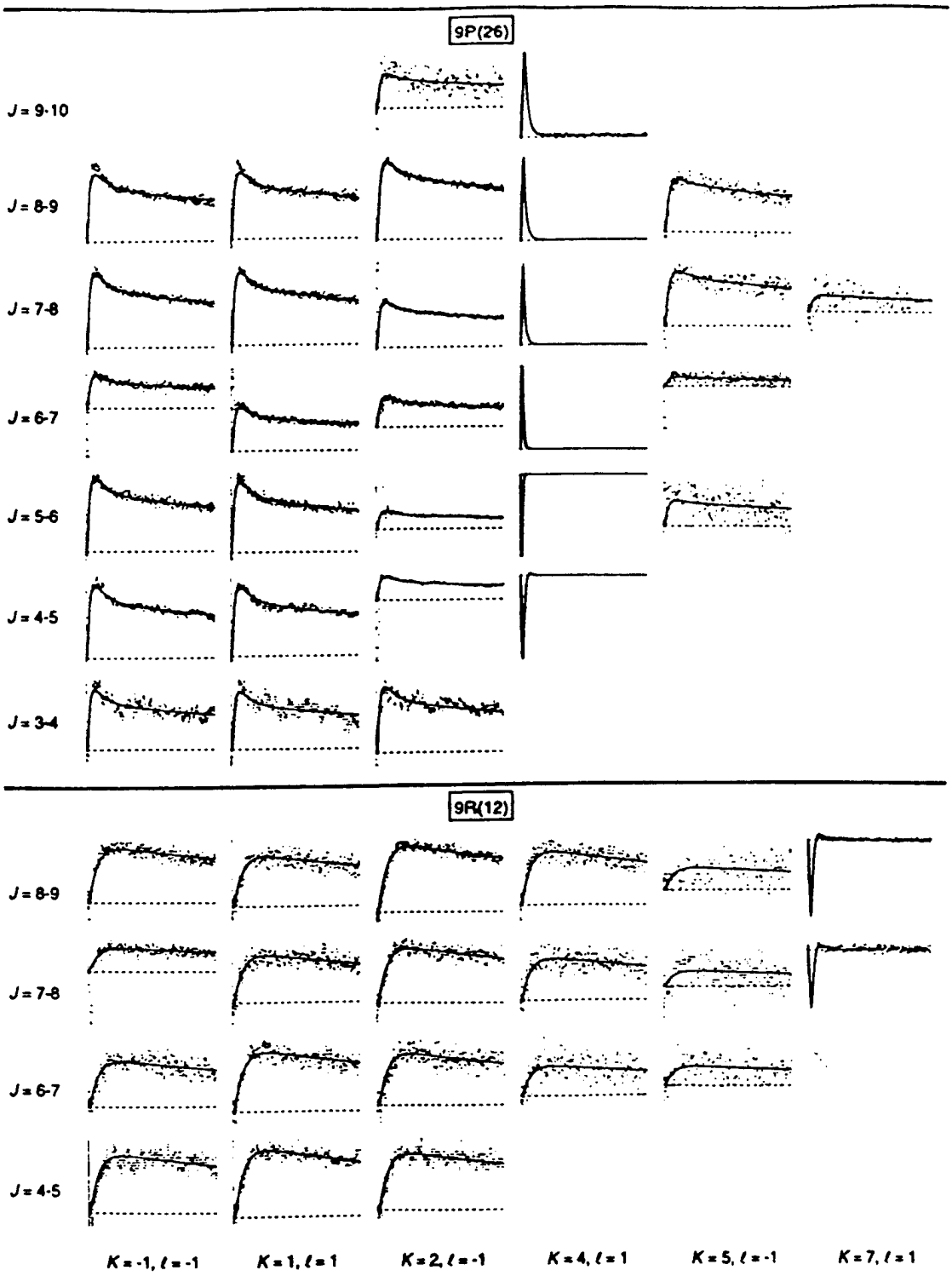

Figure III.B.2. Time resolved mm/submm probe responses for J,K transitions of the same symmetry species as the pumped transition in $CH_3{}^{35}Cl$. The 9P26 laser pumps the J = 6, K = 4, l = 1 energy level; The 9R12 laser pumps the J = 12, K = 7, l = 1 energy level.

The principal energy transfer processes among these pools and states are:

(a) The $\Delta J = n$, $\Delta K = 0$ processes; the fastest of which is the electric dipole allowed $\Delta J = 1$.

(b) The spin statistic allowed $\Delta K = 3n$ processes, which distribute any nonequilibrium pop-

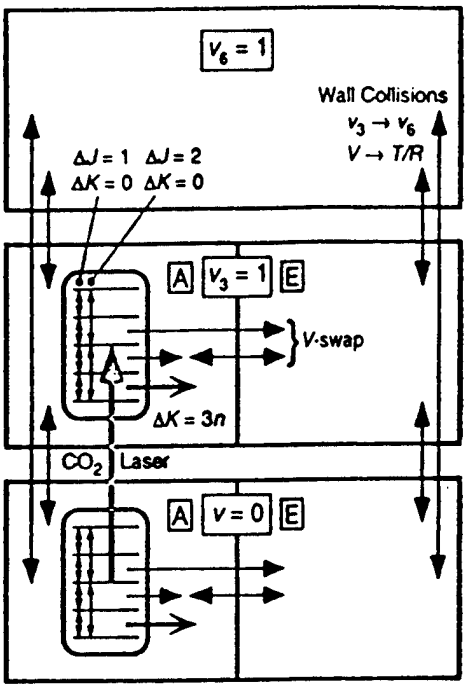

Figure III.B.3. Energy transfer model for methyl halides.

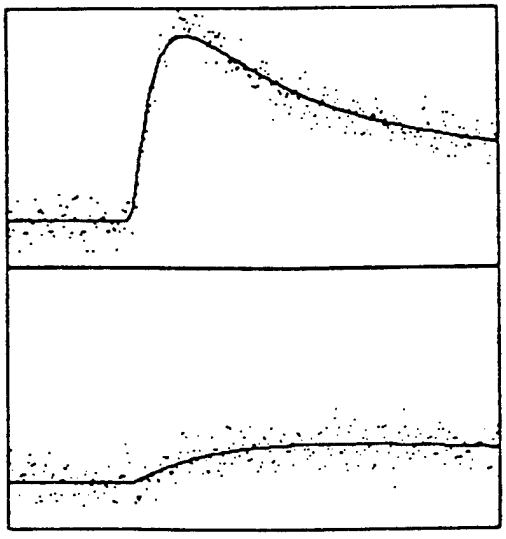

Figure III.B.4 Time resolved mm/submm probe responses (upper trace) for pool transitions of the same symmetry species (A) as the pumped transition in $^{13}CH_3F$. The lower trace shows the time response for a pool transition of the unpumped symmetry species (E).

ulation according to a thermal distribution to all other rotational states of the same symmetry.

(c) A vibrational swap process which, for example, *effectively* transfers population between the A and E symmetry species of the pumped excited vibrational state.

(d) Fast vibrational processes (e. g. $\nu_3 \rightarrow \nu_6$ or $\nu_3 + \nu_3 \rightarrow 2\nu_3$).

(e) Vibrational relaxation resulting from wall collisions.

Figure III.B.3 shows this model for CH_3F; the model for CH_3Cl is identical except for the labeling of some of the states.

2. Results: Because there are time scales and transitions for which individual processes (a) - (e) dominate, it is possible to observe these processes without benefit of deconvolution. For example, in Fig. III.B.4 pool transitions of the same symmetry as the pump are dominated by the $\Delta K = 3n$ process, while those of the other symmetry by the vibrational swap process. This separation also plays a major role in making possible an accurate deconvolution in the model of the observed data to provide meaningful physical parameters.

Table III.B.1 collects together the rotational energy transfer parameters obtained for our work to date on CH_3F and CH_3Cl. Before discussing them in more detail below, we note that: a) this small number of parameters accounts for a large and diverse set of observed state-to-state rates, b) the IOS parameters (which describe the $\Delta J = n$, $\Delta K = 0$ rates) for both species are essentially the same, and c)the $\Delta K = 3n$ rates are in the context of

Table III.B.1. Collisional Energy Transfer Rates.

		CH_3F		CH_3Cl
$\Delta K = 0$ (IOS-P)	C_σ	112. Å²		93. Å²
	γ	1.20		1.15
model		old	new	new
$\Delta K = 3n$	k_σ	137. Å²	about same	69.3 Å²
	R	fixed	similar ratio	45.8 Å²
	T_0	at 300 K	related to E_{rot}	9P(26): 145 K 9R(12): 383 K

related, but different models.

As examples, consider the rotational energy transfer processes (a) - (c).

(a) <u>The $\Delta J = n$ rates:</u> Figure III.B.2 shows for CH_3Cl the strongly nonequilibrium transitions are confined to the K stack which contains the laser pump. A similar result is obtained for CH_3F. We refer to the rates which characterize this as the $\Delta J = n$ rates. Initially, in our energy transfer model an independent, adjustable rate for each $\Delta J = n$ process was used. For the several isotopes and pumps of CH_3F and CH_3Cl, this amounted to about 25 independent parameters. Subsequently, by the use of angular momentum theory and either SPG or IOS laws, we were able to fit the calculated $\Delta J = n$ rates to two parameters for each of the species.[19,69] With this success, the IOS was included directly in the fitting routines to avoid going through the intermediary constants. This procedure has a number of advantages, not the least of which is being statistically more correct in the same spirit as was shown so elegantly in the solution of the 'oxygen problem' by Albritton *et al.*[70] Inspection of Table III.B.1 shows that the IOS parameters for both species are essentially the same. Should this be, and if so, why? Because the IOS parameters properly describe the electric dipole $\Delta J = \pm 1$ rates and because these rates are calculable from known electric dipole moments, the base C_σ constants are not really independent adjustable parameters, but rather parameters which are calculable from the known electric dipole moments. (In the results shown in Table III.B.1, the C_σ were fit for, but in other analyses in which the electric dipole rates were fixed, essentially identical results were obtained.) Additionally, the molecular geometries (which ultimately must determine the rates related to close, hard collisions which produce the larger changes in J) of the two molecules are very similar. Thus, the IOS parameters should be nearly identical because the combination of similar electric dipole moments and molecular geometries provide similar interacting molecular fields. So, once the raw time resolved data is reduced via kinetic modeling, angular momentum theory, and energy scaling laws to depend on the molecular rather than 'spectroscopic' parameters this close relationship can be shown. In contrast, the $\Delta J = n$ rates obtained directly from the kinetic model vary by well over an order of magnitude and are strong functions of J and K. This result is strong evidence that we have succeeded in describing these energy transfer processes, both simply and in terms of a small number of physically meaningful parameters.

(b) <u>The $\Delta K = 3n$ rates:</u> Inspection of Fig. III.B.2 shows that the shapes of the responses for

different J within a given K are identical for CH_3Cl; with, as discussed in (a), the exception of the states of the same K as the pumped state. This establishes that within a given K the population of the J levels can be described by a single temperature, but it does not establish that this temperature must be constant in time. However, by comparison among transitions of different K for the 9P26 pump, it can be seen that the shapes are noticeably different; indicating that the temperatures are, in fact, not constant in time. This feature, which is observed in CH_3Cl, but not CH_3F, will give rise to a simple extension of the CH_3F model.

For both isotopes of CH_3F the parameters associated with energy transfer among the pools (i. e. the $\Delta K = 3n$ and vibrational swap) are essentially the same (and, in fact, are often constrained to be the same although they are independently obtainable), as should be expected from the similar energy level structure and multipole moments of the two isotopic species. This is manifested by time resolved data having the same shape for all transitions of the respective pools.[18] In contrast, the CH_3Cl time responses shown in Fig. III.B.2 for different K but the same symmetry pool, reveal significant differences; especially the additional early time response in $|K| = 1$ with the 9P26 pump. However, by a simple, physical extension of the CH_3F model this more complex CH_3Cl experimental data can be incorporated. In the case of CH_3F, the experimental data is consistent with the simplest assumption: that the $\Delta K = 3n$ process deposits population throughout the pool according to a thermal distribution at the translational temperature (ordinarily 300 K). Although the CH_3Cl data is inconsistent with this assumption, if the temperature which describes the population transfer is described by

$$T = T_e + (T_0 - T_e)\, e^{-kt}$$

the excellent fit shown by the solid line in Fig. III.B.2 results. Here, T is the instantaneous rotational temperature of the pool, T_0 the temperature which describes the initial distribution of population, T_e the equilibrium temperature, and k the decay constant. With this, the time responses of Fig. III.B.2 are a convolution of population being transferred from the pump via the $\Delta K = 3n$ process and the varying temperature of the pool. In the case of the 9P26 pump, this favors the low energy $|K| = 1$ states at early time because of the lower initial rotational temperature. We have recently, tried refitting the CH_3F data with this extra degree of freedom of the new model. Because of the nature of the data, the manifestation of this effect is much less clear in CH_3F and families of constants lead to satisfactory fits if the CH_3F data is fit alone. It would appear that it is possible to choose a common $\Delta K = 3n$ rate for both CH_3F and CH_3Cl. If so, the difference in the appearance of the raw data would not be because of fundamentally different interaction potentials, but rather in the rotational energy level spacing of the two species.

Although the current model treats the thermalization rate as an independent variable; fundamentally it is not, clearly being related to the other rotational rates (i. e. the $\Delta K = 3n$ and $\Delta J = n$). We will return to this issue in Section IV. Here, we will briefly note that because of the much smaller B value of CH_3Cl, larger changes in J (which are restricted by multipole moment and angular momenta considerations) are required for a given change in energy; thereby making an initial distribution of population at the translational temperature more difficult to obtain.

(c) The Vibrational Swap rate: The lower trace of Figure III.B.4 shows a time response of a transition in the unpumped symmetry of CH_3F. Since these states are connected to the pump via the 'vibrational swap' process, the initial exponential rise is a direct measure of this process. This process transcends the spin statistic selection rule and *effectively* transfers population in the excited vibrational state from the symmetry species containing the pump to the other symmetry species. A very direct means of observing this rate is to simply measure the rate of population arrival in a pool state of the opposite symmetry, for example in $^{13}CH_3F$ K = 1 (K = 3 pumped) and in $^{12}CH_3F$ K = 0 (K = 2 pumped). Mahan[71] (using the results of London[72] and Margenau[73]) has shown that for cases of near resonance the cross sections for vibrational collisional energy transfer can be considerably enhanced by the presence of a large vibrational transition dipole moment such as exists in CH_3F. The related near resonance process ($\Delta E = 18\ cm^{-1}$) $\nu_3 + \nu_3 \rightarrow 2\nu_3$ has a similarly fast rate in CH_3F.[74] However, for CH_3Cl the vibrational transition dipole moment is much smaller and higher order interactions become significant. As a result the theory of Mahan is not appropriate; underestimating the 'vibrational swap' rate significantly.[69,75]

As discussed many times in this report, measurements over a range of temperatures provide both a much more stringent test of theory and lay the basis for the consideration of collisional 'spectroscopy.' Figure III.B.5 shows the measured vibrational swap rate as a function of

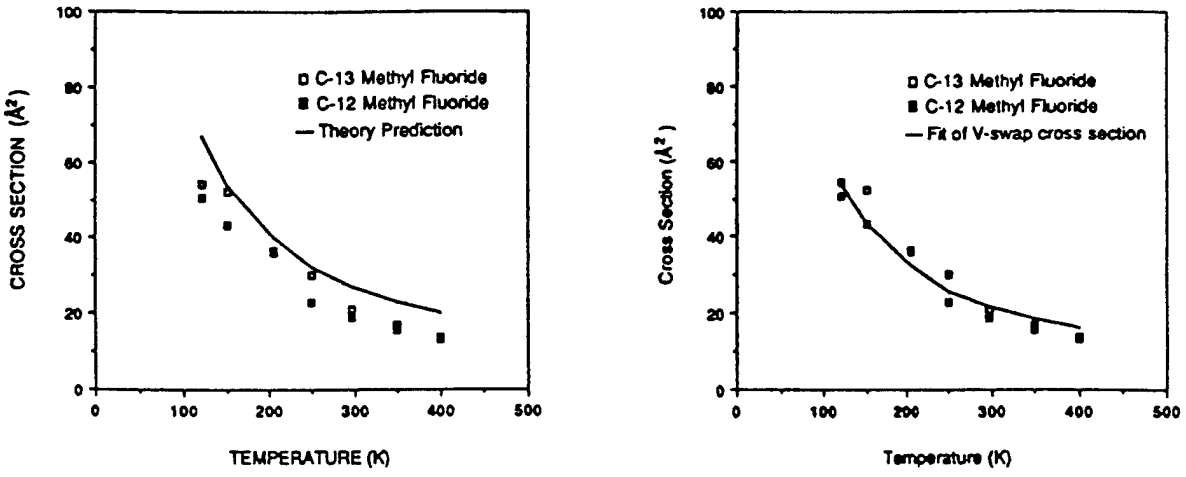

Figure III.B.5 Vibrational swap rates as a function of temperature.

temperature. The line in the left figure represents the *absolute* rate calculated from the theory of Sharma and Brau,[76] using the transition moment of Kondo *et al*. [77] The line on the figure on the right results from fitting this parameter to the data. Because this rate depends on the fourth power of the transition moment, the adjustment required for the fit is within the error bars of the constant.

3. Summary: For a very wide range of pumped transitions within several isotopic species of CH_3Cl and CH_3F a multitude of rotational energy transfer process can be described in the context of only a few molecular constants, parameters which are in general related to independently determinable parameters such as the dipole moment. This might be considered a significant achievement by the 'spectroscopy-minded' who seek to describe a seemingly unrelated set of observables in terms of a few spectroscopic constants. On the other hand, those who seek to invert the problem to learn about intermolecular interactions will be less pleased about the dearth of independent information contained in the data.

All of the results reported here have been set in the larger context of Rotational Energy Transfer by us in a recent chapter in *Advances in Atomic, Molecular, and Optical Physics*.[78]

C. Millimeter and Submillimeter Technology

In order to support our experimental activity and to contribute to the mm/submm community, our laboratory undertakes technology development as a part of its research program. Here we will briefly mention two effort in which we participate in collaboration with other research efforts in the laboratory.

We have had a long standing interest in the interaction between short (pico/femtosecond) pulses and the generation of mm/submm waves. In collaboration with John Swartz and Bob Guenther we are developing two techniques. The first uses a Ti:Sapphire laser to produce femtosecond pulses of light which in turn switch a semiconductor transmission line to generate mm/submm waves. We are especially interested in high resolution applications, based on signal processing of the demodulated optical pulse train. This work is based on our earlier work with a synchpump picosecond laser.[79] In the work covered by this report, we have shown that it is possible to generate spectroscopically useful amounts of mm/submm radiation and that the resultant radiation is of very high (~3 parts in 10^8) spectral purity.[80] The second experiment is a parasitic experiment on the bunched electron beam which drives the MKIII FEL. In this experiment significant amount of >100 GHz pulsed radiation has been produced. Here, we are both interested in the generation of radiation and the analysis of the mm/submm radiation produced as a diagnostic of the electron bunching parameters of the FEL. The diagnostic work has proven to be especially interesting and has been reported in a recent paper.[81]

In collaboration with Ron Jones and Jo Dutta of NCCU we have a related experiment which uses a microwave gun to produce an ~1 MeV beam of picosecond bunched electrons. In this dedicated experiment, interaction devices specifically designed to optimize desirable microwave source parameters (short pulses, high power, narrow bandwidth, etc.) have been used.[82]

SCIENTIFIC PERSONNEL

1. Frank C. De Lucia, Professor of Physics

2. Eric Herbst, Professor of Physics

3. Paul Helminger, Professor of Physics, University of South Alabama

4. D. D. Skatrud, Associate Professor (adjunct)

5. B. D. Guenther, Professor (adjunct)

6. Henry Everitt, Assistant Professor (adjunct)

7. John Swartz, Research Associate

8. Tom Goyette, Research Associate

9. Guo Wei, Graduate Student

10. Matthew Beaky, Graduate Student

LIST OF PUBLICATIONS

"Collisional Cooling as an Environment for Planetary Research," Thomas M. Goyette and Frank C. De Lucia, J. Geophys. Research 96, 17455 (1991).

"Millimeter- and Submillimeter-wave Spectrum of Highly Excited States of Water," J. C. Pearson, Todd Anderson, Eric Herbst, Frank De Lucia, and Paul Helminger, ApJS 379, L41-L43 (1991).

"Collisions and Rotational Spectroscopy," T. M. Goyette, R. I. McCormick, F. C. De Lucia, and H. O. Everitt, J. Mol. Spectrosc. 153, 324 (1992).

"Very Low Temperature Helium Pressure Broadening of DCl in a Collisionally Cooled Cell," Daniel R. Willey, Vi-En Choong, and Frank C. De Lucia, J. Chem. Phys. 96, 898 (1992).

"The Hydrogen Pressure Broadening at Planetary Temperatures of the 183 and 380 GHz Transitions of Water Vapor," J. M. Dutta, C. R. Jones, Thomas M. Goyette, and Frank C. De Lucia, Icarus 102, 232 (1993).

"The Temperature Dependence of Fast Vibrational Energy Transfer Processes in Methyl Fluoride," Henry O. Everitt, Frank C. De Lucia, Mol. Phys. 79, 1087 (1993).

"Variable Temperature Pressure Broadening of the $4_{1,3} - 3_{2,1}$ Transition of H_2O by O_2 and N_2," T. M. Goyette, F. C. De Lucia, J. M. Dutta, and C. R. Jones, J. Quant. Spectrosc. Radiat. Transfer 49, 485 (1993).

"The Pressure Broadening of HDO by O_2, N_2, H_2, and He between 100 and 600 K," Thomas M. Goyette, David W. Ferguson, Frank C De Lucia, J. M. Dutta, and C. R. Jones, J. Mol. Spectrosc. 162, 366 (1993).

"Time-resolved Double Resonance Study of J- and K-changing Rotational Collisional Processes in CH_3Cl," Travis W. Pape, Frank C. De Lucia, and David D. Skatrud, J. Chem. Phys. 100, 5666 (1994).

"Hydrogen and Helium Pressure Broadening of H_2S Between 2 K and 600 K," Daniel C. Flatin, J. Jerome Holton, Matthew M. Beaky, Thomas M. Goyette, and Frank C. De Lucia, J. Mol. Spectrosc. 164, 425 (1994).

"Femtosectond Demodulation Source for High Resolution Submillimeter Spectroscopy," Thomas M. Goyette, Wei Guo, Frank C. De Lucia, John Swartz, Henry O. Everitt, B. D. Guenther, and Elliott R. Brown, App. Phys. Lett. 67, 3810 (1995).

"Rotational Energy Transfer in Small Polyatomic Molecules," Henry O. Everitt and Frank C. De Lucia, Advances in Atomic, Molecular, and Optical Physics 35, 331 (1995).

"Generation of Picosecond Pulses at Millimeter Wavelengths," C. R. Jones, H. Kosai, J. M. Dutta, M. J. Peters, W. Guo, F. C. DeLucia, S. V. Benson, J. M J. Madey, J. C. Swartz, and B. D. Guenther, Appl. Phys. Lett. 67, 1483 (1995).

"Pressure Broadening of Gas Phase Molecular Ions at Very Low Temerature," J. C. Pearson, L. C. Oesterling, Eric Herbst, and F. C. DeLucia, Phys. Rev. Lett. 75, 2940 (1995).

"Nondestructive Diagnostics for Relativistic Picosecond Bunched Electron Beams," J. C. Swartz, B. D. Guenther, F. C. De Lucia, Wei Guo, C. R. Jones, H. Kosai, and J. M. Dutta, Phys. Rev. E 52, 5416 (1995).

"Hydrogen and Helium Pressure Broadening of CH_3F between 1 K and 600 K," Matthew M. Beaky, Daniel C. Flatin, J. Jerome Holton, Thomas M. Goyette, and Frank C. De Lucia, J. Mol. Struct. 352/353, 245 (1995).

1. W. C. King and W. Gordy, Phys. Rev. **90**, 3139 (1953).
2. P. Helminger, F. C. De Lucia, and W. Gordy, Phys. Rev. Lett. **25**, 1397 (1970).
3. P. Helminger, J. K. Messer, and F. C. De Lucia, Appl. Phys. Lett. **42**, 309 (1983).
4. R. A. Booker, R. L. Crownover, F. C. De Lucia, J. Mol. Spectrosc. **128** , 62 (1988).
5. D. R. Willey, R. L. Crownover, D. N. Bittner, F. C. De Lucia, J. Chem. Phys. **89**, 1923 (1988).
6. D. R. Willey, D. N. Bittner, and F. C. De Lucia, J. Mol. Spectrosc. **133**, 182 (1989).
7. J. K. Messer and F. C. De Lucia, Phys. Rev. Lett. **53**, 2555 (1984).
8. D. R. Willey, D. N. Bittner, and F. C. De Lucia, Mol. Phys. **67**, 455 (1989).
9. F. C. De Lucia, G. A. Blake, P. Helminger, and E. Herbst, J. Chem. Phys. **78**, 2312 (1983).
10. H. E. Warner, W. T. Conner, R. H. Petrmichl, and R. C. Woods, J. Chem. Phys. **81**, 2514 (1984).
11. G. A. Blake, K. B. Laughlin, R. C. Cohen, K. L. Busarow, and R. J. Saykally, Ap. J. **316**, L45 (1987).
12. M. Bogey, C. Demuynck, M. Denis, J. L. Destombes, and B. Lemoine, Astron. and Astrophys. **137**, L15 (1984).
13. M. Winnewisser , private communication.
14. G. Plummer, private communication.
15. D. D. Skatrud and F. C. De Lucia, Appl. Phys. Lett. **46**, 631 (1985).
16. R. I. McCormick, H. O. Everitt, F. C. De Lucia, and D. D. Skatrud, IEEE J. Quant. Electron. **QE-23**, 2069 (1987).
17. R. I. McCormick, F. C. De Lucia, and D. D. Skatrud, IEEE J. Quant. Electron., **QE-23**, 2060 (1987).
18. H. O. Everitt and F. C. De Lucia, J. Chem. Phys. **90**, 3520 (1989).
19. H. O. Everitt and F. C. De Lucia, J. Chem. Phys. **92**, 6480 (1990).
20. H. O. Everitt and F. C. De Lucia, Mol. Phys. **79**, 1087 (1993).
21. D. R. Willey, R. L. Crownover, D. N. Bittner, and F. C. De Lucia, J. Chem. Phys. **89**, 6147 (1988).
22. D. R. Willey, D. N. Bittner, and F. C. De Lucia, J. Mol. Spectrosoc. **134** , 240 (1989).
23. D. R. Willey, D. N. Bittner, and F. C. De Lucia, Mol. Phys. **66**, 1 (1988).
24. D. R. Willey, T. M. Goyette, W. L. Ebenstein, D. N. Bittner, and F. C. De Lucia, J. Chem. Phys. **91**, 122 (1989).
25. D. N. Travis, J. C. McGurk, D. McKeown, R. G. Denning, Chem Phys. Lett. **45**, 287 (1977).
26. P. B. Davies and A. J. Morton-Jones, Appl. Phys. **B42**, 35 (1987).
27. T. A. Brunner and D. Pritchard, Ad. Chem. Phys. **50**, 589 (1982).
28. E. H. Putley, Infrared Physics **4**, 1 (1964).
29. P. Helminger, F. C. De Lucia, and W. Gordy, Phys. Rev. Lett. **25**, 1397 (1970).
30. D. R. Willey, V. -E. Choong, and F. C. De Lucia, J. Chem. Phys. **96**, 898 (1992).
31. J. M. Dutta, C. R. Jones, T. M. Goyette, and F. C. De Lucia, Icarus **102**, 232-239 (1993).
32. T. M. Goyette and F. C. De Lucia, J. Mol. Spectrsoc. **143**, 346 - 358 (1990).
33. T. M. Goyette, D. W. Ferguson, F. C. De Lucia, J. M. Dutta, and C. R. Jones, J. Mol. Spectrosc. **162**, 366 (1993).
34. J. M. Dutta, C. R. Jones, T. M. Goyette, and F. C. De Lucia, Icarus **102**, 232 (1993).
35. T. M. Goyette, J. M. Dutta, and C. R. Jones, JSQRT **49**, 485 (1993).
36. D. C. Flatin, J. J. Holton, M. M. Beaky, T. M. Goyette, and F. C. De Lucia, J. Mol. Spectrosc. **164**, 425 (1994).
37. R. D. Levine, B. R. Johnson, J. T. Muckerman, and R. B. Bernstein, J. Chem. Phys. **49**, 56 (1968).
38. W. Erlewein, M. von Seggern, and J. P. Toennies, Z. Physik **211**, 35 (1968).
39. M. von Seggern and J. P. Toennies, Z. Physik. **218**, 341 (1969).
40. A. Palma and S. Green, J. Chem. Phys. **85**, 1333 (1986).
41. A. Von Engel, *Ionized Gases* (Oxford University, London, 1955).

42. J. C. Pearson, L. C. Oesterling, E. Herbst, and F. C. De Lucia, Phys. Rev. Lett. **75**, 2940 (1995).
43. L. S. Rothman, R. R. Gamache, A. Goldman, L. R. Brown, R. A Toth, H. M. Pickett, R. L. Poynter, J. -M. Flaud, C. Camy-Peyret, A. Barbe, N. Husson, C. P. Rinsland, and M. A. H. Smith, Appl. Opt. **26**, 4058 (1987).
44. J. H. Van Vleck and V. F. Weisskopf, Ref. Mod. Phys. **17**, 227-236 (1945).
45. P. W. Anderson, Phys. Rev. **76**, 647 (1949).
46. C. H. Townes and A. L. Schawlow, "Microwave Spectroscopy," McGraw-Hill, New York, 1955.
47. S. Green and L. D. Thomas, J. Chem. Phys. **73**, 5391 (1980).
48. S. Green, National Resource for Computation in Chemistry Soft ware Catalogue (Lawrence Berkeley Laboratory, Berkeley, CA 1980).
49. S. Green, J. Chem. Phys. **82**, 4548 (1985).
50. J. O. Hirschfelder, C. F. Curtiss, and R. B. Bird, "Molecular Theory of Gases and Liquids," Wiley, New York, 1954.
51. H. O. Everitt, D. D. Skatrud, and F. C. De Lucia, Appl. Phys. Lett. **49**, 16 (1986).
52. T. Oka, in *Ad. in At. Mol. Phys.* **9**, 127, Academic Press, New York, 1973.
53. A. P. Cox, G. W. Flynn, and E. B. Wilson, Jr., J. Chem. Phys. **46**, 3262 (1967).
54. A. M. Ronn and E. B. Wilson, Jr. J. Chem. Phys. **46**, 3262 (1967).
55. L. Frenkel, H. Marantz, and T. Sullivan, Phys. Rev. **A3**, 1640 (1971).
56. P. J. Seibt, J. Chem. Phys. **57**, 1343 (1972).
57. H. Jetter, E. F. Pearson, C. L. Norris, J. C. McGurk, and W. H. Flygare, J. Chem. Phys. **59**, 1796(1973).
58. S. Kano, T. Amano, and T. Shimizu, J. Chem. Phys. **64**, 4711 (1976).
59. W. A. Kreiner, A. Ever, and H. Jones, J. Mol. Spectrosc. **52**, 420 (1974).
60. E. N. Chesnokov and V. N. Panfilov, Sov. Phys. JETP **46**, 1112 (1977).
61. L. Laux, B. Foy, D. Harradine, and J. I. Steinfeld, J. Chem. Phys. **80**, 3499 (1984).
62. D. Harradine, B. Foy, L. Laux, M. Dubs, and J. I. Steinfeld, J. Chem. Phys. **81**, 4267 (1984).
63. J. G. Haub and B. J. Orr, J. Chem. Phys. **86**, 3380 (1987).
64. F. Menard-Bourcin and L. Doyennette, J. Chem. Phys. **88**, 5506 (1988).
65. B. Foy, J. Hetzler, G. Millot, and J. I. Steinfeld, J. Chem. Phys. **88**, 6838 (1988).
66. U. Shin and R. H. Schwendeman, J. Chem. Phys. **91**, 3966 (1989).
67. B. Abel, S. L. Coy, J. J. Klaassen, and J. I. Steinfeld, J. Chem. Phys. **96**, 8236 (1992).
68. W. H. Matteson and F. C. De Lucia, IEEE J. Quant. Electron. **QE-19**, 1284 (1983).
69. T. Pape, F. C. De Lucia, and D. D. Skatrud, submitted for publication.
70. D. L. Albritton, W. J. Harrop, A. L. Schmeltekopf, and R. M. Zare, J. Mol. Spectrsoc **46**, 103 (1973).
71. B. H. Mahan, J. Chem. Phys. **46**, 98 (1967).
72. F. London, Z. Phys. **63**, 245 (1930).
73. H. Margenau, Rev. Mod. Phys. **11**, 1 (1939).
74. R. S. Sheorey and G. W. Flynn, J. Chem. Phys. **72**, 1175 (1980).
75. H. O. Everitt, unpublished Ph.D. thesis, Duke University.
76. R. D. Sharma and C. A Brau, J. Chem. Phys. **50**, 924 (1969).
77. S. Kondo, Y. Koga, and T. Nakanaga, J. Phys. Chem. **90**, 1519 (1986).
78. H. O. Everitt and F. C. De Lucia, in *Advances in Atomic, Molecular, and Optical Physics* **35**, 331 (1995).
79. F. C. De Lucia, B. D. Guenther, and T. Anderson, Appl. Phys. Lett. **47**, 894 (1985).
80. T. M. Goyette, W. Guo, F. C. De Lucia, J. Schwartz, H. O. Everitt, B. D. Guenther, and E. R. Brown, Appl. Phys, Lett. **67**, 3810 (1995).
81. J. C. Schwartz, B. D. Guenther, F. C. De Lucia, W. Guo, C. R. Jones, H. Kosai, and J. M. Dutta, Phys. Rev. E**52**, 5416 (1995).
82. C. R. Jones, H. Kosai, J. M. Dutta, M. J. Peters, W. Guo, F. C. De Lucia, S. V. Benson, J. M. J. Madey, J. C. Swartz, and B. D. Guenther, Appl. Phys. Lett. **67**, 1483 (1995).